JOURNAL OF GUIDANCE, CONTROL, AND DYNAMICS
Vol. 33, No. 1, January–February 2010

Effects of Heave Washout Settings in Aircraft Pitch Disturbance Rejection

D. M. Pool,* P. M. T. Zaal,† M. M. van Paassen,‡ and M. Mulder§
Delft University of Technology, 2600 GB Delft, The Netherlands

DOI: 10.2514/1.46351

In most moving-base flight simulators, the simulated aircraft motion needs to be filtered with motion washout filters to keep the simulator within its limited motion envelope. Translational motion in particular requires filtering, as the low-frequency components of the vehicle motion tend to quickly drive simulators toward their motion bounds. Commonly, linear washout filters are therefore used to attenuate the simulated motion in magnitude and in phase. It is found in many studies that the settings of these washout filters affect pilot performance and control behavior. In most of these studies, no comparison to a case with one-to-one motion cues is performed as a result of the limited motion envelope of the simulators used. In the current study, an experiment was performed in the SIMONA Research Simulator at the Delft University of Technology to investigate the effects of heave washout settings on pilot performance and control behavior in a pitch attitude control task. In addition to rotational pitch motion, heave accelerations at the pilot station that result directly from aircraft pitch were evaluated. This heave motion component could be supplied one-to-one in the simulator due to the modest size of the aircraft model, a Cessna Citation I business jet. The experiment revealed that pilot performance and control activity both increased significantly with increasing heave motion fidelity. An analysis of pilot control behavior using pilot models indicated that the enhanced performance was caused by an increase in the magnitude with which pilots responded to visual and physical motion stimuli and a decrease in the amount of visual lead that was generated by the pilots.

Nomenclature

A	=	sinusoid amplitude, deg
$a_{z_{cg}}$	=	c.g. heave acceleration, m s^{-2}
a_{z_θ}	=	pitch-heave acceleration, m s^{-2}
e	=	tracking error signal, deg
f_d	=	disturbance forcing function, deg
f_t	=	target forcing function, deg
H_{nm}	=	neuromuscular system dynamics
H_{ol}	=	open-loop response
H_{sc}	=	semicircular canal dynamics
H_{p_e}	=	pilot visual response
$H_{p_{a_z}}$	=	pilot heave motion response
H_{p_θ}	=	pilot pitch motion response
$H(j\omega)$	=	frequency response function
$H(s)$	=	transfer function
H_{θ,δ_e}	=	controlled system dynamics
j	=	imaginary unit, -
K	=	gain, -
K_m	=	motion perception gain, -
K_v	=	visual perception gain, -
k	=	sinusoid index, -
l	=	pitch-heave arm length, m
N	=	number of points, -
n	=	forcing function frequency integer factor, -
S	=	power spectral density
s	=	Laplace variable
T_I	=	visual lag time constant, s
T_L	=	visual lead time constant, s
T_{sc_1}, T_{sc_2}, T_{sc_3}	=	semicircular canal model time constants, s
t	=	time, s
u	=	pilot control signal, deg
z	=	vertical position, m

Symbols

δ_e	=	elevator deflection, deg
ζ	=	damping factor, -
ζ_{nm}	=	neuromuscular damping, -
θ	=	pitch angle, deg
σ^2	=	variance
τ_m	=	motion perception time delay, s
τ_v	=	visual perception time delay, s
ϕ	=	sinusoid phase shift, rad
φ_m	=	phase margin, deg
ω	=	frequency, rad s^{-1}
ω_c	=	crossover frequency, rad s^{-1}
ω_{nm}	=	neuromuscular frequency, rad s^{-1}
ω_{sp}	=	short period frequency, rad s^{-1}

Subscripts

d	=	disturbance
mf	=	motion filter
t	=	target

Presented as Paper 6241 at the AIAA Modeling and Simulation Technologies Conference, Chicago, IL, 10–13 August 2009; received 15 July 2009; revision received 16 September 2009; accepted for publication 16 September 2009.

*Ph.D. Candidate, Control and Simulation Division, Faculty of Aerospace Engineering, P.O. Box 5058; d.m.pool@tudelft.nl. Student Member AIAA.

†Ph.D. Candidate, Control and Simulation Division, Faculty of Aerospace Engineering, P.O. Box 5058; p.m.t.zaal@tudelft.nl. Student Member AIAA.

‡Associate Professor, Control and Simulation Division, Faculty of Aerospace Engineering, P.O. Box 5058; m.m.vanpaassen@tudelft.nl. Member AIAA.

§Professor, Control and Simulation Division, Faculty of Aerospace Engineering, P.O. Box 5058; m.mulder@tudelft.nl. Senior Member AIAA.

I. Introduction

COMPARED to aircraft, flight simulators are severely limited in their motion envelope. This causes the generation of motion cues in flight simulation to be an inevitable compromise between the desired level of motion cue fidelity and the available motion

space. Since the 1970s [1], it has become common practice to use washout algorithms for transforming aircraft rotational and linear accelerations to simulator motion. Such washout algorithms typically use linear high- and low-pass filters to attenuate simulated aircraft motion states, both in magnitude (scaling) and in phase (washout). In addition to the attenuation of the real aircraft motions, the washout performed by motion filters is also known to result in false motion cues [2].

Numerous studies in literature have shown that simulator washout filter settings affect pilot perception and acceptance of simulator motion [3–8]. In addition, it has been shown that the design and tuning of motion washout filters is heavily dependent on the maneuver that is to be simulated [9]. Therefore, insight into the effects of the rotational and linear motion components involved in a specific maneuver and their effect on pilot motion perception and control behavior is required for proper motion washout filter design. To achieve the optimal level of simulator motion fidelity, those motion components that provide important feedback to the pilot must be replicated at high accuracy, whereas those that are less likely to affect pilots' control behaviors can be attenuated to save valuable simulator motion space.

An example of a piloting task, for which this relative importance of the different perceivable motion components is of interest, is a manual aircraft pitch attitude stabilizing task. Zaal et al. [10] describe an experiment in which the effects of two different vertical motion components on pilot control behavior in a pitch attitude disturbance-rejection task have been investigated, which they referred to as pitch-heave and c.g. heave. The first results from the fact that pilots are generally seated well in front of the aircraft center of pitch rotation and that rotational pitch accelerations therefore cause correlated vertical (heave) accelerations at the pilot station. In addition, changes in pitch attitude cause vertical motion of the aircraft c.g., which yields a second component of the total heave motion. The results described in [10] indicate that, because similar information can be deduced from rotational pitch motion and the pitch-heave motion component, pilot control behavior is affected by both these motion cues in a similar way.

The effects of pitch-heave on pilot performance and control behavior found by Zaal et al. [10] were, however, significantly lower in magnitude than those of rotational pitch motion. In that experiment, pitch motion was presented one to one, as it would rarely exceed plus or minus 5 deg, but the heave motion was filtered using a third-order linear high-pass filter. This motion filter was required for attenuating the high-magnitude low-frequency c.g. heave motion and, to allow for fair comparison of both heave motion components, was also used to filter the pitch-heave accelerations. The relatively lower magnitude of the effects of pitch-heave may therefore be partly explained by the heave motion filter used in this experiment.

This paper describes an investigation into the effects of heave washout filter settings on pilot control behavior in the same pitch tracking task as was studied by Zaal et al. [10]. By varying the parameters of the heave washout filter, some insight into the effects of the gain and phase attenuation induced by such linear filters on pilot skill-based control behavior can be obtained. Because of the significant correlation between pitch and pitch-heave motion during aircraft pitch maneuvering, it can be anticipated that the effects of degrading heave motion cues by washout will have less impact when pitch motion is also present.

In this paper, first, some of the details of the pitch attitude disturbance-rejection task will be described and, using data from [10], the effect of the washout filter adopted in this previous experiment on the supplied heave motion cues will be illustrated. Then, the setup of the current human-in-the-loop experiment that was performed in the SIMONA Research Simulator (SRS) at the Delft University of Technology will be described in detail. In this experiment, different heave motion attenuation settings were tested to allow for evaluation of the effects of heave washout on pilot control behavior. Objective measurements of pilot control behavior from the current experiment will be presented and compared with results of the experiment described in [10]. This paper ends with a discussion and conclusions.

II. Heave Motion During Pitch Maneuvering

During aircraft pitch maneuvering, pilot motion sensation will not consist solely of physical pitch rotation. Because of aircraft geometry and dynamical responses, some additional linear motion will also be perceivable: most notably vertical heave motion. In this section, the heave motion cues associated with aircraft pitch control, the heave motion filter, and some of the main trends that were observed in the experiment described by Zaal et al. [10] will be discussed.

A. Heave Motion Components

As indicated in Fig. 1, in [10] a distinction is made between two components of the total vertical motion at the pilot station. The first, referred to as pitch-heave motion and indicated with the symbol a_{z_θ} in Fig. 1, represents the vertical motion that is a direct result of the pitch rotation and the distance between the pilot station and the c.g. l. A second contribution to the vertical motion a pilot perceives during pitch maneuvering, referred to as c.g. heave ($a_{z_{cg}}$), results from changes in aircraft altitude that are caused by the changes in aircraft pitch. Note that this breakdown into vertical motion of the aircraft c.g. and heave motion with respect to the c.g. could alternatively have been performed using the instantaneous center of pitch rotation as described in [11]. However, due to the modest size of the aircraft considered in this study, a Cessna Citation I, the difference between both definitions is small.

The two distinct components of heave motion identified in [10] yield highly different motion sensations at the pilot station. For pure pitching maneuvers, the pitch-heave accelerations are linearly related to the second derivative of the aircraft pitch attitude through

$$a_{z_\theta} = -l\ddot{\theta} \tag{1}$$

As indicated by this relation, the pitch-heave component of the vertical motion at the pilot station essentially provides a vertical presentation of the aircraft's pitching motion. For a Cessna Citation I, the distance between the aircraft c.g. and the pilot station is approximately 3.2 m. As a result, the magnitude of this heave motion component is relatively modest (for pitch attitudes between ± 5 deg, only ± 0.28 meters of vertical motion space would be required for one-to-one presentation of the pitch-heave motion).

The pitch-heave accelerations a_{z_θ} are a high-pass response to elevator control inputs. The c.g. heave component of the vertical motion, however, is a high-magnitude low-pass response to an elevator input. As changes in aircraft altitude are typically in the order of meters, one-to-one presentation of this component of vertical motion is not possible in most full-motion flight simulators. The analysis of pilot control behavior described in [10] revealed that pilot control behavior during pitch tracking was affected by both pitch-heave and c.g. heave motion. The investigation of the effects of heave washout on pilot control behavior described in this paper, however, requires a baseline condition in which heave motion is presented one to one. Therefore, the c.g. heave component of the vertical linear motion during pitch maneuvering could not be considered in the current study.

B. Heave Motion Filter

A linear high-pass heave motion filter, as typically adopted in motion base flight simulators, was used for attenuating the aircraft heave motion in the experiment described in [10]. To achieve

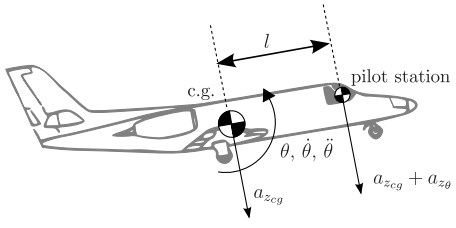

Fig. 1 Aircraft motion cues at the c.g. and pilot station during a pitch maneuver.

significant low-frequency attenuation, a third-order high-pass filter was used, for which the transfer function is given by

$$H_{\mathrm{mf}}(s) = K_{\mathrm{mf}} \frac{s^2}{s^2 + 2\zeta_{n_{\mathrm{mf}}}\omega_{n_{\mathrm{mf}}}s + \omega_{n_{\mathrm{mf}}}^2} \frac{s}{s + \omega_{b_{\mathrm{mf}}}} \tag{2}$$

In Eq. (2), K_{mf} represents the motion filter gain, which was set to 0.6. The filter break frequencies $\omega_{n_{\mathrm{mf}}}$ and $\omega_{b_{\mathrm{mf}}}$ and the damping factor $\zeta_{n_{\mathrm{mf}}}$, which together define the dynamical characteristics of the washout filter, were fixed to 1.25 rad/s, 0.3 rad/s, and 0.7, respectively.

This washout filter was required for attenuation of the c.g. heave component of the total vertical motion but not for the pitch-heave motion component. Despite the fact that pitch-heave motion could be replicated one to one for the Citation I aircraft used in the [10] experiment, both heave motion components were attenuated by the washout filter of Eq. (2) to allow for fair comparison of their respective effects on pilot control behavior during pitch tracking.

Figure 2 depicts the frequency response of the high-pass filter of Eq. (2). In addition, the average spectrum of the aircraft pitch-heave accelerations measured by Zaal et al. [10] for their seven subjects is shown alongside (circles indicate disturbance signal frequencies). Note the high-pass characteristic of the pitch-heave accelerations. Furthermore, observe that the motion filter corner frequencies were chosen such that the main filter amplitude attenuation did not affect the frequencies for which the pitch-heave acceleration had the most power. Finally, note from Fig. 2 that both filter break frequencies were also selected to be significantly below the short period frequency of the Citation dynamics $\omega_{\mathrm{sp}} = 2.759$ rad/s.

Figure 2 suggests that when the pitch-heave accelerations are attenuated by the motion filter defined by Eq. (2), the resulting motion cues will not have been attenuated much in the frequency range in which they hold the most power. This is further illustrated by the top graph in Fig. 3, which shows a comparison of unfiltered and filtered pitch-heave acceleration time traces. Note that the gain attenuation of 0.6 is clearly visible, but hardly any phase shift is observable from the acceleration time traces. As illustrated by the bottom graph of Fig. 3, this no longer holds when the acceleration signals are integrated to vertical position, as the washout clearly reduces the magnitude of the simulator excursions.

C. Observed Effects of Heave

One of the main findings of the experiment described in [10] was that rotational pitch motion and translational pitch-heave motion were found to have highly similar effects on pilot performance and control behavior during pitch tracking. As the pitch-heave acceleration component is directly related to pitch acceleration through Eq. (1), this was hypothesized before the experiment was performed. The magnitude of the effects of a_{z_θ} on pilot control behavior and

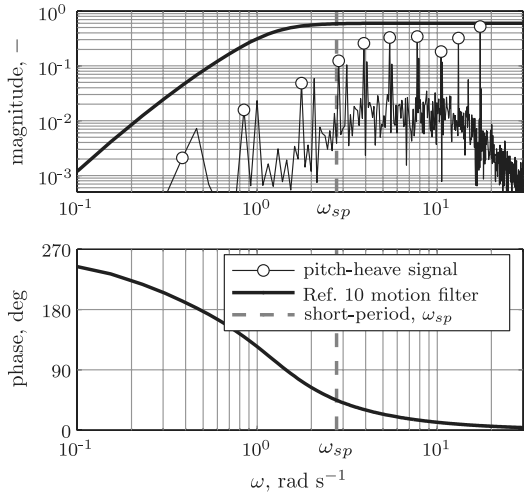

Fig. 2 Average pitch-heave acceleration spectrum compared with frequency response of [10] heave motion filter.

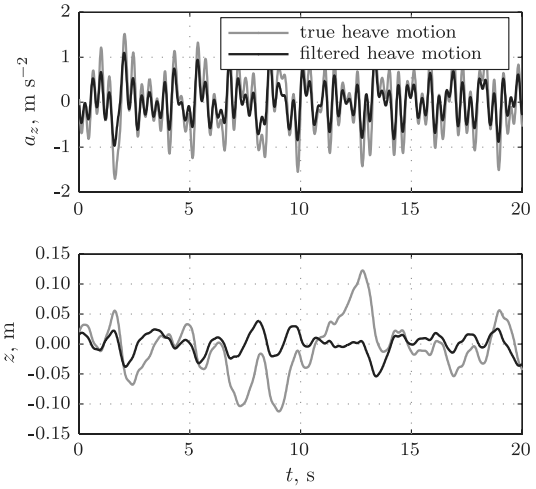

Fig. 3 Comparison of sample heave acceleration and displacement time traces for true and filtered heave motion ([10] motion filter).

performance were, however, found to be significantly lower than those observed for rotational pitch motion. This is illustrated in Fig. 4, in which the time-domain variances of the tracking error signal and the pilot control signal are depicted as measures of pilot performance and control activity, respectively.

Figure 4 clearly illustrates that both tracking performance and control activity were found to increase when rotational pitch motion was made available (the lower σ_e^2 signifies better tracking performance). In addition, note the similar but reduced effect of the addition of pitch-heave motion, which is most clearly observed for the error variance data shown in Fig. 4a. Highly similar trends were visible in the underlying pilot control behavior. From the analysis of the motion filter used by Zaal et al. [10] for their experiment, this reduced magnitude of the effects of pitch-heave motion compared with rotational pitch motion is believed to be at least partly due to the use of this motion filter. This warrants more research into the effect of motion washout filters on pilot control behavior in attitude control tasks.

III. Experiment

An experiment was performed on the SRS at the Delft University of Technology to investigate the influence of heave motion attenuation on pilot control behavior in a pitch tracking task. This section describes the experimental method and hypotheses. The control task, experimental procedures, and apparatus of the current experiment are equal to those of the experiment described in [10] to allow for valid comparison of both sets of results.

A. Method

1. *Aircraft Pitch Control Task*

To investigate the effects of heave motion attenuation on pilot behavior during aircraft pitch control, control behavior was evaluated

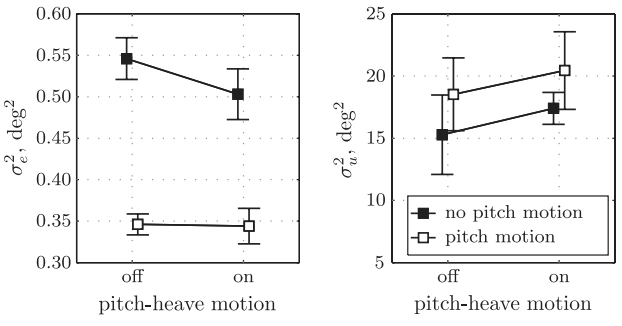

a) Tracking error variance **b) Control variance**

Fig. 4 Effects of pitch and pitch-heave motion on tracking performance and control activity (data from [10]).

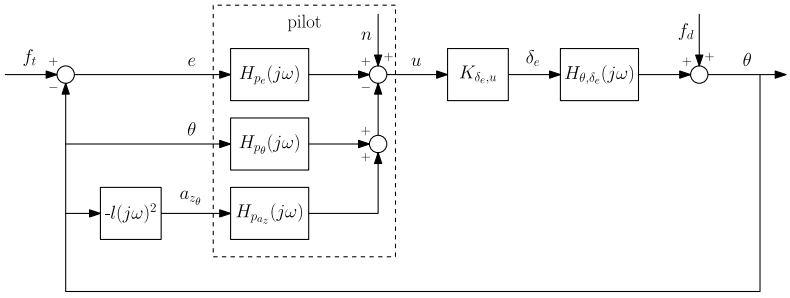

Fig. 5 Schematic representation of a closed-loop pitch control task with pitch and pitch-heave motion cues.

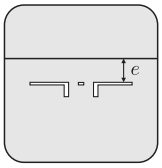

Fig. 6 Compensatory display.

in the pitch control task depicted in Fig. 5. In this task, a pilot controls the pitch angle θ of the controlled element by compensating for deviations from the desired pitch attitude by minimizing the tracking error e, as shown on a compensatory display (Fig. 6). In addition to this visual information, continuous feedback of physical pitch and pitch-heave motion is available. This yields a pilot response, which is a summation of a visual response $H_{p_e}(j\omega)$, a pitch motion response $H_{p_\theta}(j\omega)$, a pitch-heave motion response $H_{p_{a_z}}(j\omega)$, and a remnant signal n that accounts for the nonlinear behavior.

The controlled dynamics for the pitch attitude control task are the elevator to pitch attitude dynamics of a Cessna Citation I Ce500, linearized at an altitude of 10,000 ft and an airspeed of 160 kt. The transfer function of this controlled element is given by

$$H_{\theta,\delta_e}(s) = -10.6189\frac{s + 0.9906}{s(s^2 + 2.756s + 7.612)} \tag{3}$$

The control input scaling gain $K_{\delta_e,u}$, which defined the scaling of stick deflections to model elevator inputs, was set to -0.2865 to yield optimal control authority. To induce pitch attitude tracking errors that pilots need to compensate for, target and disturbance forcing function signals (denoted with the symbols f_t and f_d in Fig. 5, respectively) were inserted into the closed-loop system, as shown in Fig. 5. These forcing function signals were constructed as quasi-random sum-of-sines signals, also used in many previous research efforts [12–16]. The same target and disturbance signals (as adopted by Zaal et al. [10]) were also used for this experiment, yielding a control task in which the disturbance-rejection element was dominant. The sum-of-sines signals were constructed according to

$$f_{d,t}(t) = \sum_{k=1}^{N_{d,t}} A_{d,t}(k)\sin[\omega_{d,t}(k)t + \phi_{d,t}(k)] \tag{4}$$

where the subscripts d and t indicate the disturbance or target forcing function, respectively. In Eq. (4), $A(k)$, $\omega(k)$, and $\phi(k)$ indicate the amplitude, frequency, and phase of the kth sine in f_d or f_t. N indicates the number of sines in the signals. The properties of the sine components of both forcing function signals are given in Table 1.

2. *Independent Variables*

This study aims to investigate the effects of heave washout settings on the usefulness of the pitch-heave component of heave motion during pitch attitude disturbance-rejection. As for the control task described in Sec. III.A.1, no washout filter is in fact required for replicating the pitch-heave accelerations a_{z_θ} in the SRS; the effects of a linear washout filter in heave can be compared with a full-motion case. Five different heave washout settings will be considered in this experiment. The motion filter gains and break frequencies for these five experimental conditions are depicted graphically in Fig. 7.

Heave conditions K0.0 and K1.0 represent conditions with no-heave motion and one-to-one heave motion, respectively. The combination of heave filter break frequency and gain that was used for the experiment described in [11] is depicted by condition F0.6. Heave filter F1.0 has the same break frequency as used for F0.6 but has unity gain. K0.6 has the same gain as condition F0.6 but with a break frequency of zero. These conditions are expected to reveal if a possible reduction in usefulness of the heave motion is a result of the gain attenuation K_{mf} or of the phase shifts induced by the washout, for which the impact can be characterized by the value of the break frequencies $\omega_{n_{\text{mf}}}$ and $\omega_{b_{\text{mf}}}$.

The properties of the five heave filters used in the experiment are summarized in Table 2. All five heave conditions will be performed with and without the presence of one-to-one rotational pitch motion cues, as an interaction between heave filter settings, and the availability of pitch motion is anticipated. This means a total of 10 conditions were performed in the experiment.

3. *Dependent Measures*

A number of dependent measures from the experiment were considered to be of interest. First of all, the variances of the recorded error signal e and control signal u were calculated as measures of tracking performance and control activity in the time domain, respectively. In addition, a multimodal pilot model, defined in detail in Sec. III.A.4, was fit to the time-domain data using a genetic

Table 1 Experiment forcing function properties

	Disturbance, f_d				Target, f_t		
n_d, -	ω_d, rad s^{-1}	A_d, deg	ϕ_d, rad	n_t, -	ω_t, rad s^{-1}	A_t, deg	ϕ_t, rad
5	0.383	0.344	−1.731	6	0.460	0.698	1.288
11	0.844	0.452	4.016	13	0.997	0.488	6.089
23	1.764	0.275	−1.194	27	2.071	0.220	5.507
37	2.838	0.180	4.938	41	3.145	0.119	1.734
51	3.912	0.190	5.442	53	4.065	0.080	2.019
71	5.446	0.235	2.274	73	5.599	0.049	0.441
101	7.747	0.315	1.636	103	7.900	0.031	5.175
137	10.508	0.432	2.973	139	10.661	0.023	3.415
171	13.116	0.568	3.429	194	14.880	0.018	1.066
226	17.334	0.848	3.486	229	17.564	0.016	3.479

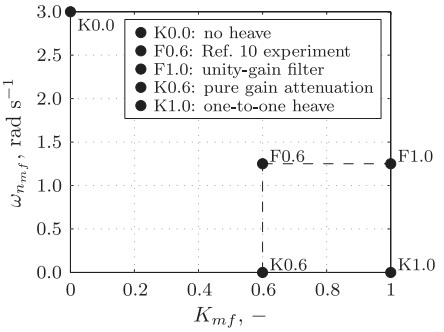

Fig. 7 Graphical representation of heave motion filter conditions.

maximum likelihood (MLE) procedure [17]. To evaluate the accuracy of the pilot model in the time domain, the variance accounted for (VAF) was calculated using the measured pilot control signal and the output of the linear pilot model [18]. The changes in pilot-model parameters were used to quantify changes in pilot control strategy for the different attenuations of heave motion. The performance of the attenuation of the disturbance and target errors was evaluated by calculating the crossover frequencies and phase margins of the disturbance and target open-loop response, respectively.

4. *Pilot Model*

The structure of the quasi-linear pilot model used in this study is shown in Fig. 5. It consists of parallel linear responses to all perceived visual and physical motion cues supplemented with a remnant signal n to account for all nonlinearities. The model of the pilot visual response, given by Eq. (5), is based on the work of McRuer et al. [12] and was shown to be suitable for modeling pilot control of the aircraft dynamics defined in Eq. (3) in [19]:

$$H_{p_e}(j\omega) = K_v \frac{(1 + T_L j\omega)^2}{1 + T_I j\omega} e^{-j\omega\tau_v} H_{nm}(j\omega) \tag{5}$$

In Eq. (5), K_v and τ_v represent the pilot visual gain and visual perception time delay, respectively. The visual equalization characteristic is defined using the lead and lag constants, T_L and T_I. The neuromuscular actuation dynamics are included through the neuromuscular system model $H_{\mathrm{nm}}(j\omega)$, which is assumed to be a second-order mass-spring-damper system:

$$H_{\mathrm{nm}}(j\omega) = \frac{\omega_{\mathrm{nm}}^2}{(j\omega)^2 + 2\zeta_{\mathrm{nm}}\omega_{\mathrm{nm}} j\omega + \omega_{\mathrm{nm}}^2} \tag{6}$$

The dynamics of the neuromuscular system are characterized with the second-order eigenfrequency and damping factor ω_{nm} and ζ_{nm}, which are both free parameters of the pilot model. The pilot model for the no-motion condition of the experiment (F0.0, without pitch motion) consisted solely of Eqs. (5) and (6).

In literature, pilot responses to physical motion cues have often been described with models that included only contributions from the human vestibular motion sensors [10,15,16], that is, the semicircular canals for rotational motion and the otoliths for linear motion (specific forces). Pilot vestibular motion responses to rotational motion have, for instance, been modeled successfully as

$$H_{p_\theta}(j\omega) = K_m (j\omega)^2 H_{\mathrm{sc}}(j\omega) e^{-j\omega\tau_m} H_{\mathrm{nm}}(j\omega) \tag{7}$$

Table 2 Heave motion filter settings

Condition	K_{mf}, -	$\omega_{n_{\mathrm{mf}}}$, rad s^{-1}	$\omega_{b_{\mathrm{mf}}}$, rad s^{-1}	$\zeta_{n_{\mathrm{mf}}}$, -
K0.0	0	——	——	——
F0.6	0.6	1.25	0.3	0.7
F1.0	1	1.25	0.3	0.7
K0.6	0.6	——	——	——
F1.0	1	——	——	——

for numerous previous human-in-the-loop experiments [10,15,16,18,20–22]. In Eq. (7), K_m and τ_m are the pilot motion response gain and time delay, respectively. The frequency response function $H_{\mathrm{sc}}(j\omega)$, with $T_{\mathrm{sc}_1} = 0.11$ s, $T_{\mathrm{sc}_2} = 5.9$ s, and $T_{\mathrm{sc}_3} = 0.005$ s, represents the response of the human semicircular canals to rotational acceleration inputs, as described in [16]:

$$H_{\mathrm{sc}}(j\omega) = \frac{1 + T_{\mathrm{sc}_1} j\omega}{(1 + T_{\mathrm{sc}_2} j\omega)(1 + T_{\mathrm{sc}_3} j\omega)} \tag{8}$$

Equation (7) describes a pilot's response to rotational motion from a physical perspective by making use of knowledge of the underlying physical motion perception processes. Because of the fact that the semicircular canals are sensitive to rotational accelerations and that their dynamics are a single integrator in the frequency range of interest for human manual vehicular control, the model defined by Eq. (7) effectively provides additional pilot lead (i.e., a response to rotational velocity) in parallel to the lead generated from the visual response [Eq. (5)]. Despite the fact that the otoliths are sensitive to specific forces and yield a sensation of linear acceleration [16], pilots are known to integrate these sensed accelerations to rates during manual control tasks to yield a lead contribution that is highly similar to that obtained from the semicircular canals [23].

This additional lead from the vestibular sensors is often stated to be superior to a visual lead due to the lower perceptual latency [16]. Previous experiments, which investigated control behavior in control tasks similar to the one depicted in Fig. 5, have indeed shown that pilots substitute lead from physical motion stimuli (if available) for the lead generated from visual information [10,22]. For the experiment described in this paper, it is hypothesized that this additional lead information is present in both the rotational pitch motion and the vertical pitch-heave motion. Therefore, the contribution of the pitch and heave motion channels of the pilot model were combined. To achieve this, both motion response channels are defined to take the form of a pure lead with a time delay on the pitching motion:

$$H_{p_\theta}(j\omega) = K_m j\omega e^{-j\omega\tau_m} H_{\mathrm{nm}}(j\omega) \tag{9}$$

$$H_{p_{a_z}}(j\omega) = \frac{-1}{l(j\omega)^2} H_{p_\theta}(j\omega) = \frac{-K_m}{lj\omega} e^{-j\omega\tau_m} H_{\mathrm{nm}}(j\omega) \tag{10}$$

For conditions with only heave motion, Eq. (10) (which includes the distance between the c.g. and the pilot station l) is included in the pilot model. For conditions in which pitch motion is present (including those with additional heave), only Eq. (9) is used for modeling the pilot motion response. This approach allows for comparison of the pilot-model parameters that are of interest (mainly the visual lead constant T_L and the motion gain K_m) over all conditions of the experiment. A validation of this modeling approach will be given in Sec. IV.C.1 using experimental data.

5. *Apparatus*

The experiment was performed in the SRS at the Delft University of Technology (see Fig. 8). Pitch and heave motion cues were generated with the a six degree-of-freedom SRS motion system, which consisted of six hydraulic actuators in a hexapod configuration. The SRS motion system latency is 30 ms [24].

Subjects were seated in the right pilot seat. The compensatory visual display shown in Fig. 6 was depicted on the right primary flight display in the SRS cockpit. The time delay associated with the generation of visual images on the cockpit displays has been determined to be around 20–25 ms [25].

A sidestick with electrical control loading was used to give control inputs to the controlled aircraft dynamics, see Eq. (3). The sidestick was defined to have no breakout force and a maximum pitch axis deflection of ± 14 deg. The stick roll axis was kept fixed at the zero position. The stiffness of the stick was set to 1.1 N/ deg for stick deflections under 9 deg and to 2.6 N/ deg for larger stick excursions.

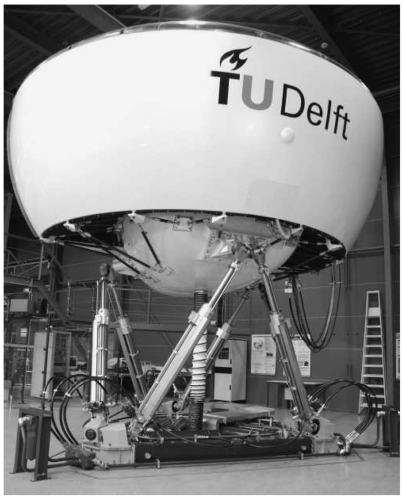

Fig. 8 The SRS.

6. Participants and Experimental Procedures

Seven subjects participated in the experiment. All participants were male, and their ages ranged from 23 to 47 years old. Four of the participants had experience as pilots of single- or multi-engine aircraft. The others had extensive experience with manual vehicle control tasks from previous human-in-the-loop experiments. Before the start of the experiment, the participants were briefed on the objective of the experiment and the experimental method. The main instruction to the subjects was to minimize the pitch tracking error e, presented on the visual display, within their capabilities. After the end of each experiment run, the subjects were informed of their score in order to motivate them to perform at their maximum level of performance.

The experiment had a balanced Latin square design; that is, the conditions were presented in quasi-random order. The subjects were trained on the task until they performed at a stable level of performance. When five repetitions of each condition had been collected at a stable performance level, the experiment was terminated. No fixed number of training runs was defined before the experiment. On average, 9 to 10 repetitions of each experimental condition were sufficient to gather the measurement data. Typically, each subject performed 16 runs; that is, two repetitions of all conditions in between breaks. This allowed each subject to complete the experiment in approximately 4 h.

An individual experiment run was defined to last 90 s, of which the final 81.92 s were used as the measurement data. The first 8.08 s of data from each run were discarded for analysis to remove the initial transient response resulting from the pilots stabilizing the system dynamics. Data were logged at a frequency of 100 Hz.

B. Hypotheses

Based on the experiment described in [10] and other experiments on the effects of motion attenuation on pilot performance and control behavior [26,27], some hypotheses can be formulated. Filtering pitch-heave motion is hypothesized to yield lower tracking performance. This decrease is expected to be less when rotational pitch motion is also present. As both types of motion give the same information, the pitch motion then compensates for the lower fidelity pitch-heave motion.

For the pilot-model parameters, it is hypothesized that, as the fidelity of the motion is increased, the visual and physical motion perception gains will increase. In addition, the visual lead is thought to decrease, as the additional motion cues provide a more efficient source of lead information. The disturbance crossover frequency is thought to increase, accompanied by a decrease in disturbance phase margin. For the target crossover frequency and phase margin, the opposite trend to the disturbance crossover frequency and phase margin is anticipated when motion fidelity is increased. Furthermore, it is hypothesized that one-to-one pitch-heave motion affects pilot performance and control behavior in the same order of magnitude as one-to-one rotational pitch motion.

IV. Results

This section presents the results of the human-in-the-loop experiment. First, the effects of variation of pitch and heave motion on tracking performance and control activity are presented. Second, pilot-vehicle system crossover frequency and phase margin (with respect to both the disturbance and target signals used in the control task) are presented as measures of combined pilot-vehicle system stability and bandwidth. Finally, changes in pilot control behavior over the different motion conditions are analyzed explicitly using the multimodal pilot model, introduced in Sec. III.A.4. The statistical significance of the results is identified, where possible, using a two-way repeated measures analysis of variance (ANOVA) that considers effects of pitch and heave motion cues separately.

A. Tracking Performance and Control Activity

Figure 9 depicts the mean tracking performance and control activity (expressed in terms of the variances of the error and control signals e and u) for the ten conditions of the experiment. Black data points indicate measurements for conditions without pitch motion; data from the corresponding heave motion conditions with additional pitch motion are depicted with white squares. Variance bars indicate the 95% confidence intervals of the means for each condition over the seven experiment subjects. For calculation of the confidence intervals, the data were corrected for between-subject effects. Repeated measures ANOVA results for the data depicted in Fig. 9 are summarized in Table 3.

From Fig. 9a, a clear difference in achieved tracking performance for runs with and without pitch motion can be observed. This

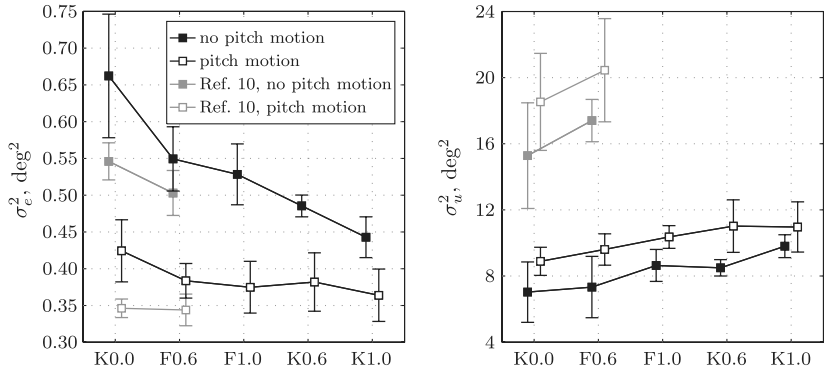

a) Tracking error variance **b) Control variance**

Fig. 9 Mean tracking performance and control activity for different heave motion filter settings.

Table 3 Two-way repeated measures ANOVA results for tracking performance and control activity, where ** is highly significant ($p < 0.05$) and - is not significant ($p \geq 0.1$)

Independent variables	Dependent measures					
	σ_e^2			σ_u^2		
Factor	df	F	Sig.	df	F	Sig.
Pitch	1, 6	41.15	**	1, 6	9.24	**
Heave	1.3, 8.0[a]	22.24	**	1.6, 9.8[a]	6.95	**
Pitch × heave	4, 24	10.74	**	4, 24	1.22	-

[a]Greenhouse–Geisser sphericity correction applied.

decrease in σ_e^2 when pitch motion cues were available is a highly significant effect [$F(1, 6) = 41.15$, $p < 0.05$]. In addition, heave motion fidelity was also found to affect control task performance significantly [$F(1.3, 8.0) = 22.24$, $p < 0.05$], as increased heave motion fidelity clearly yielded lower error signal variances. Note, from Table 1, that Mauchly's test indicated a violation of the sphericity assumption for the main effect of heave on σ_e^2, and that the conservative Greenhouse–Geisser correction was applied.

The effect of heave motion settings on tracking performance is found to be significantly reduced when pitch motion cues are also available. Addition of heave motion is still found to increase performance, but the effect is much smaller than for the corresponding conditions without pitch. This reduced effect of heave motion fidelity for conditions with pitch motion is also evident from the significant interaction found for both types of motion cues from the ANOVA [$F(4, 24) = 10.74$, $p < 0.05$].

Figure 9b clearly shows increased control activity, both with increased heave fidelity and when additional pitch motion cues are made available. These effects of pitch and heave on σ_u^2 are both significant: $F(1, 6) = 9.24$, $p = 0.023$ and $F(1.6, 9.8) = 6.95$, $p = 0.016$, respectively. In addition, the increase in control activity with increasing heave fidelity is found to be more or less equal in magnitude (with and without availability of pitch motion), which is also supported by the insignificant interaction between pitch and heave motion found for σ_u^2, $F(4, 24) = 1.22$, $p = 0.33$.

The gray data shown in Fig. 9 depict the error and control signal variances measured during the [10] experiment for the K0.0 and F0.6 heave motion conditions, which were shared by both experiments. Note that the observed trends between these conditions are highly similar for both sets of data, but that the average tracking performance for these shared conditions was clearly better during the previous experiment than found from the current data. Average control activity is also found to be markedly higher for the data from [10]. To illustrate the origin of this discrepancy, average tracking performance and control activity for the K0.0 and F0.6 conditions from the current experiment are depicted in Fig. 2 alongside the individual subject data from [10], shown in gray.

Figure 10 clearly illustrates that three subjects who performed the [10] experiment can be characterized as achieving above average tracking performance (low σ_e^2) and adopting a comparatively high-gain control strategy (high σ_u^2). The data measured during the current experiment nicely coincide with the data from the remaining participants of the previous experiment. For the current experiment, a more homogeneous group of subjects was used, as all of them were comparatively low-gain controllers. Note that, despite the clear offset in the data of the different participants in Fig. 10, the observed trends are remarkably consistent for all subjects, especially for the error signal variance σ_e^2. This same consistency was also observed for the data from the current experiment.

B. Pilot-Vehicle System Crossover Frequency and Phase Margin

As indicated in Sec. III.A.1, the control task studied in this experiment was a combined disturbance-rejection and target following task in which the disturbance-rejection element was made dominant by downscaling the target forcing function signal. For such a combined task, the suppression of tracking errors induced by both forcing function signals determines overall closed-loop system performance. The crossover frequencies and phase margins of the open-loop response functions with respect to both target and disturbance signals can give an indication of pilot-vehicle system performance and stability [4]. These target and disturbance open-loop response functions can be calculated from time-domain measurements according to [10]

$$H_{\mathrm{ol},d}(j\omega_d) = -\frac{S_{u,f_d}(j\omega_d)}{S_{\delta_e,f_d}(j\omega_d)}, \qquad H_{\mathrm{ol},t}(j\omega_t) = \frac{S_{\theta,f_t}(j\omega_t)}{S_{e,f_t}(j\omega_t)} \tag{11}$$

In Eq. (11), the symbol $S_{x,y}$ indicates the cross power spectral density function of the signals x and y. Figure 11 depicts the average crossover frequencies and phase margins that have been determined from $H_{\mathrm{ol},d}$ and $H_{\mathrm{ol},t}$. The error bars again indicate the 95% confidence intervals of the means for each condition over the seven subjects. Furthermore, for calculation of the 95% confidence intervals, subject means of the data shown in Fig. 11 have been corrected in order to account for between-subject effects. Table 4 summarizes the ANOVA results for the crossover data depicted in Fig. 11. Data from [10] are shown in gray for reference. Note again the offset between the data from both experiments, which reflects the influence of the subjects with high-gain control strategies in the gray data.

First of all, note from Fig. 11 and Table 4 that the presence of pitch motion significantly affects both target and disturbance loop crossover frequencies and phase margins. A clear increase in $\omega_{c,d}$ of approximately 1 rad/s is observed when pitch motion is made available [$F(1, 6) = 176.15$, $p < 0.05$], which is accompanied by a significant reduction of disturbance loop phase margin $\varphi_{m,d}$ [$F(1, 6) = 23.40$, $p < 0.05$] of around 10 deg. Pitch motion cues are found to induce the opposite changes in the target open-loop

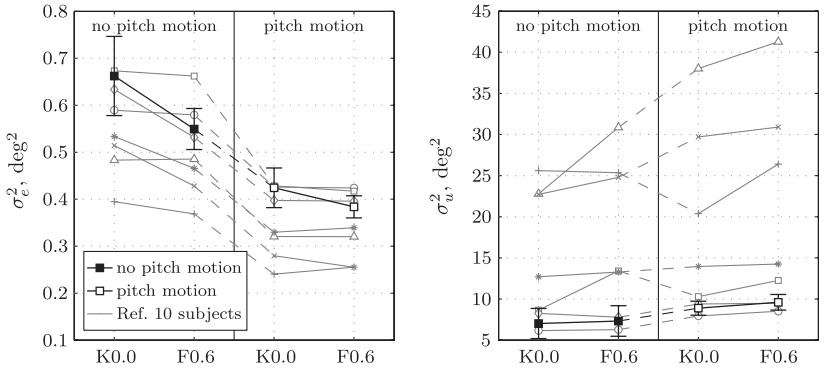

a) Tracking error variance **b) Control variance**

Fig. 10 Comparison of mean tracking performance and control activity during current experiment with individual subject data from [10] for identical motion conditions for different heave motion filter settings.

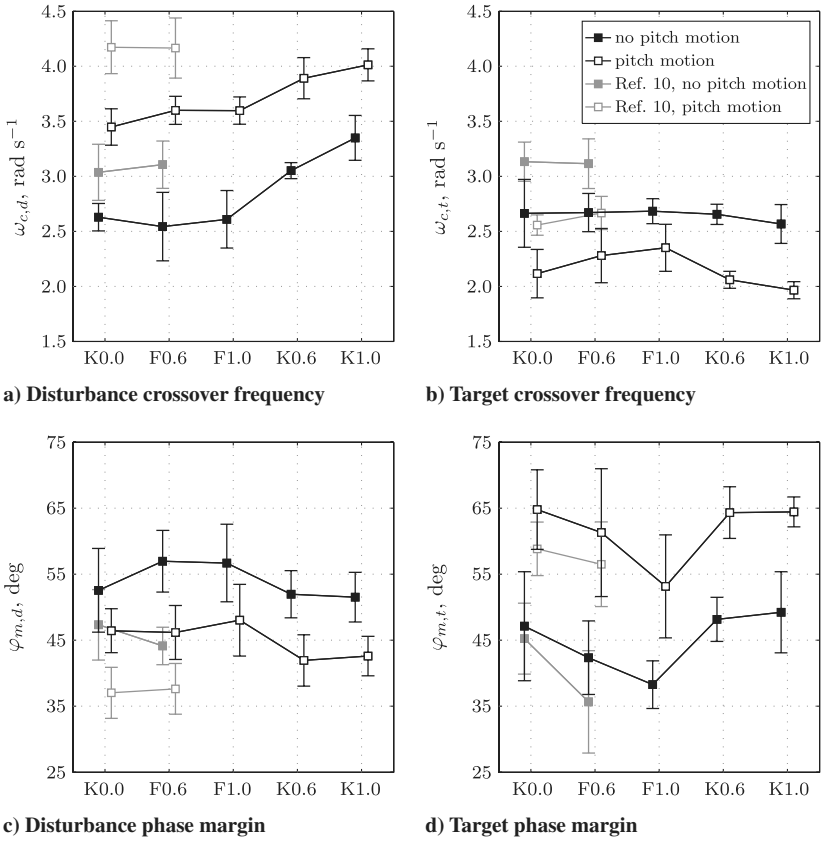

Fig. 11 Mean disturbance and target loop crossover frequency and phase margin for different heave motion filter settings.

response function; a significant decrease in crossover frequency [$F(1, 6) = 40.37$, $p < 0.05$] and a significant increase in phase margin [$F(1, 6) = 24.49$, $p < 0.05$] are observed in Figs. 11b and 11d, respectively.

The variation in heave motion cues over the different experimental conditions also induced some significant changes in the crossover frequencies and phase margins, shown in Fig. 11. Table 4 indicates that the increase in disturbance crossover frequency with increasing heave motion fidelity observed in Fig. 11a is statistically significant [$F(4, 24) = 24.52$, $p < 0.05$]. Similar to the effects of pitch motion observed previously, a marginally significant decreasing trend in disturbance phase margin [$F(4, 24) = 2.78$, $p = 0.05$] is also observed. Note that, compared with the no-heave conditions (K0.0), $\omega_{c,d}$ and $\varphi_{m,d}$ are not significantly different for the washout conditions F0.6 and F1.0, both with and without pitch motion. Rather, the sharp changes in disturbance crossover frequency and phase margin for the conditions where heave motion without washout was present (K0.6 and K1.0) are the cause of the significant main effects, listed in Table 4.

The target loop crossover frequency is found to be significantly less affected by varying levels of heave motion fidelity than $\omega_{c,d}$. A slight decreasing trend is observed with increasing heave fidelity (mainly for the conditions for which pitch motion was available in addition to unfiltered heave), but this effect is only marginally significant [$F(1.8, 10.5) = 3.34$, $p = 0.08$]. The target phase margin is seen to decrease when filtered heave motion cues are made available (K0.6) and reduces even further when the filter gain is increased to unity (K1.0). For the conditions at which heave motion was presented without washout, $\varphi_{m,t}$ is seen to increase again to roughly the same level as when no-heave motion was available. As can be verified from Table 4, this is a highly significant effect [$F(1.7, 10.4) = 9.06$, $p < 0.05$].

As is clearly visible from Fig. 11, the trends in target and disturbance loop crossover frequency and phase margin observed for the different levels of heave motion fidelity appear to be independent of the availability of additional pitch motion. This observation is supported by the ANOVA results, listed in Table 4, as the interaction of pitch and heave shows no significant effects on any of the crossover parameters. For the disturbance crossover frequency, this interaction is close to statistically significant [$F(4, 24) = 2.44$, $p = 0.074$]; however, it can be explained by the fact that the increase in $\omega_{c,d}$ with heave motion fidelity appears slightly larger when pitch motion is not available.

Finally, note that all main trends in target and disturbance loop crossover frequency and phase margin with the addition of pitch and heave motion cues, as shown in Fig. 11 (that is, an overall increase in

Table 4 Two-way repeated measures ANOVA results for crossover data, where ** is highly significant ($p < 0.05$), * is significant ($0.05 \leq p < 0.1$), and - is not significant ($p \geq 0.1$)

Independent variables	Dependent measures											
	$\omega_{c,d}$			$\varphi_{m,d}$			$\omega_{c,t}$			$\varphi_{m,t}$		
Factor	df	F	Sig.	df	F	Sig.	df	F	Sig.	df	F	Sig.
Pitch	1, 6	176.15	**	1, 6	23.40	**	1, 6	40.37	**	1, 6	24.49	**
Heave	4, 24	24.52	**	4, 24	2.78	*	1.8, 10.5[a]	3.34	*	1.7, 10.4[a]	9.06	**
Pitch × heave	4, 24	2.44	*	4, 24	0.83	-	4, 24	1.15	-	4, 24	0.40	-

[a]Greenhouse–Geisser sphericity correction.

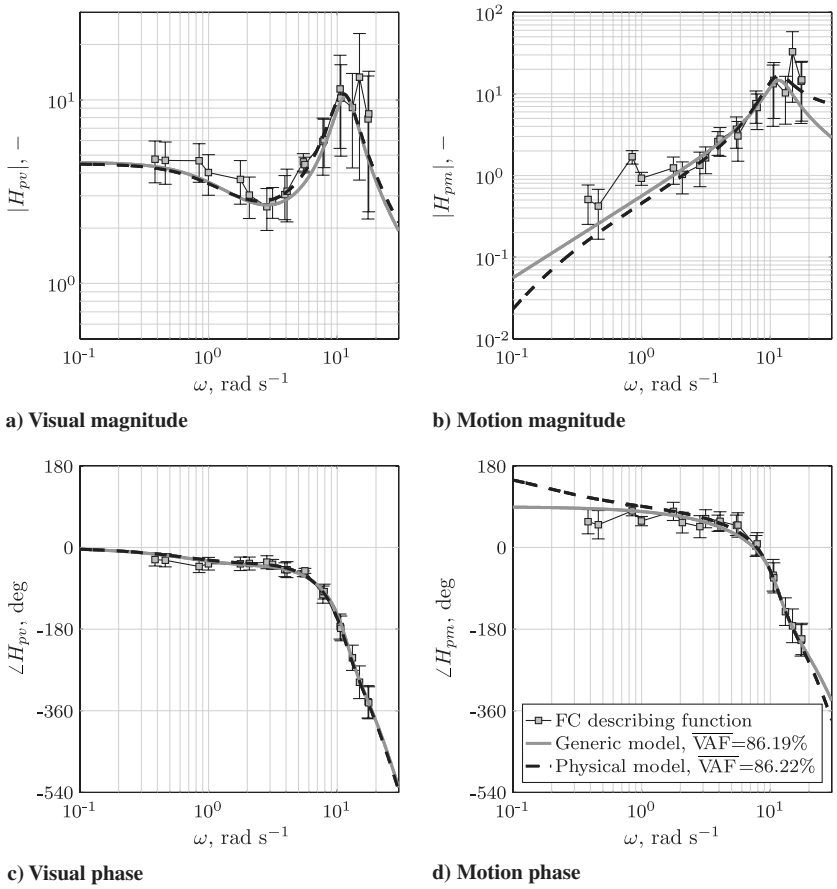

a) Visual magnitude **b) Motion magnitude**

c) Visual phase **d) Motion phase**

Fig. 12 Comparison of generic and physical pilot model fits for the experimental condition with pitch motion and no heave motion (K0.0).

$\omega_{c,d}$ and $\varphi_{m,t}$ and a corresponding decrease in $\omega_{c,t}$ and $\varphi_{m,d}$), are highly similar to findings from other experiments [10,15,16,22,28].

C. Pilot Modeling Results

The marked variation in crossover frequencies and phase margins described in Sec. IV.B hints at significant changes in pilot control behavior over the different motion conditions. To quantify these possible shifts in pilot control strategy, a multimodal pilot model has been fit to the measurement data using a time-domain MLE estimation technique [17].

1. Pilot-Model Validation

The use of the generic model given by Eqs. (9) and (10) for describing pilot response to pitch and heave motion cues is a simplification compared with physical models, as the one defined by Eq. (7). Figure 12 shows average pilot-model frequency responses that were estimated for the condition with only pitch motion (pitch motion, K0.0) for both the physical and generic pilot motion response models. The visual response model was that of Eq. (5) for both model fits. In addition to these model frequency responses, pilot describing functions calculated using a Fourier coefficients (FC) estimation method [29] are shown for reference.

Figure 12 clearly shows that the generic pilot model provides a fit to the measurement data that is highly comparable with the fit of the physical model. The difference in VAF for both models is less than 0.1%. The VAF is a measure often used in system identification for indicating the percentage of the variance in the measured model output signal that can be explained by the model in [18]. This small difference in VAF for both models depicted in Fig. 12 indicates that they perform equally well in describing the measured pilot control signal for the condition with only pitch motion. For modeling pilot heave motion responses, similar negligible differences were found between using a physical model (which included otolith dynamics) and the generic model of Eq. (10).

To further illustrate the accuracy of the pilot modeling approach adopted in this paper, Fig. 13 depicts the mean pilot-model VAF for all conditions of the experiment. Figure 13 shows that the linear part of the pilot model is able to describe around 86% of the variance in the control signal u, and therefore provides an accurate fit, for all conditions. The slightly decreased VAF found for the conditions with the unity gain washout filter (F1.0) suggests slightly decreased linearity of pilot control behavior for this condition. This may have been caused by the high gain on the filtered heave cues in this condition that made the desired heave motion, but also the false cues generated by the washout, more perceivable.

2. Pilot-Model Parameter Estimates

Figure 14 depicts the mean pilot-model parameter estimates for all 10 conditions of the experiment. The error bars indicate the 95% confidence intervals of the means taken over all seven participants of the experiment. The repeated measures ANOVA results are given in

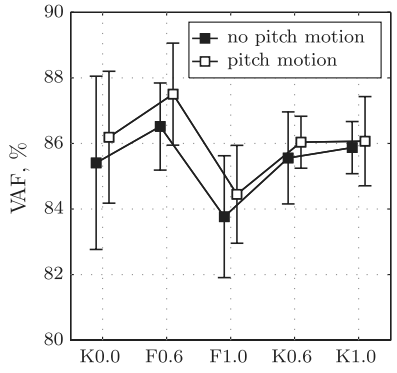

Fig. 13 Mean pilot-model VAF for different heave motion filter settings.

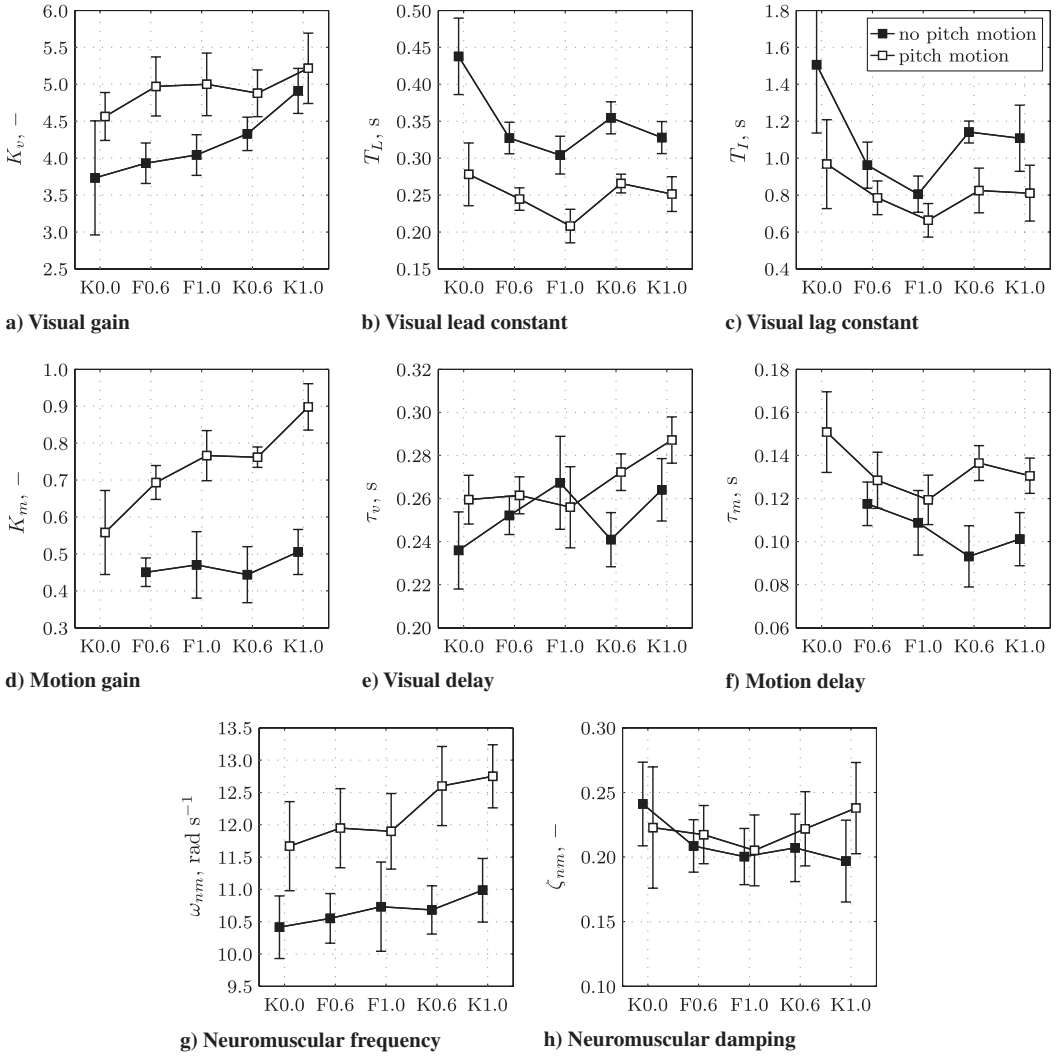

a) Visual gain **b) Visual lead constant** **c) Visual lag constant**

d) Motion gain **e) Visual delay** **f) Motion delay**

g) Neuromuscular frequency **h) Neuromuscular damping**

Fig. 14 Mean pilot-model parameters for different heave motion filter settings.

Tables 5 and 6. Note that the two-way repeated measures ANOVA used to analyze all other dependent measures could not be performed for the pilot-model motion gain K_m and time delay τ_m because these parameters are not available for the no-motion condition. For these two parameters, a one-way repeated measures ANOVA was performed instead with a single factor (motion) that had nine levels.

Figure 14a shows that the pilot visual gain K_v was found to increase both when pitch motion was made available and with an increasing level of heave fidelity. As can be verified from Table 5, both of these effects were found to be statistically significant: $F(1, 6) = 14.60$, $p < 0.05$ and $F(4, 24) = 6.89$, $p < 0.05$, respectively. In addition, Fig. 14a clearly shows the reduced effect of heave fidelity on K_v if pitch motion is also present. This interaction between pitch and heave motion was also found to be significant: $F(4, 24) = 3.24$, $p = 0.029$.

The pilot visual lead and lag time constants (see Figs. 14b and 14c) show highly similar trends over the different conditions of the experiment. Such apparent coupling between T_L and T_I has also been observed in earlier experiments [10]. The visual lead time constant is found to decrease significantly if pitch motion cues are available [$F(1, 6) = 51.01$, $p < 0.05$]. A generally decreasing trend in T_L is also visible with increasing heave fidelity, which is also found to be highly significant [$F(4, 24) = 29.21$, $p < 0.05$]. Finally, a statistical significant interaction was found for T_L [$F(4, 24) = 5.11$, $p < 0.05$], which is caused by the comparatively high value of the visual lead constant for the no-motion condition. The effects of pitch and heave motion on the lag time constant T_I were found to be similar to those found for T_L but slightly less statistically significant (see Table 5). A high-pass motion filter, as defined by Eq. (2), introduces some phase lead on the supplied heave accelerations (see Fig. 2).

Table 5 Two-way repeated measures ANOVA results for visual channel model parameters, where ** is highly significant ($p < 0.05$) and * is significant ($0.05 \leq p < 0.1$)

Independent variables	Dependent measures											
	K_v			T_L			T_I			τ_v		
Factor	df	F	Sig.	df	F	Sig.	df	F	Sig.	df	F	Sig.
Pitch	1, 6	14.60	**	1, 6	51.10	**	1, 6	17.26	**	1, 6	10.43	**
Heave	4, 24	6.89	**	4, 24	29.21	**	1.2, 7.2[a]	11.24	**	4, 24	5.73	**
Pitch × heave	4, 24	3.24	**	4, 24	5.12	**	4, 24	3.26	*	4, 24	4.45	**

[a]Greenhouse–Geisser sphericity correction.

Figures 14b and 14c clearly show that the visual lead and lag constants are found to be markedly lower for the conditions with heave washout (that is, F0.6 and F1.0) than for the equivalent conditions without washout (K0.6 and K1.0). This marked decrease in the amount of visual lead pilots generated for conditions F0.6 and F1.0 seems to indicate that the presence of a high-pass washout filter reduces the amount of visual lead compensation required from pilots for stable attitude control and thereby clearly affects their adopted control strategy.

The identified values for the pilot motion gain, shown in Fig. 14d, clearly show an increase in K_m when pitch motion is made available. In addition, K_m is found to increase further with increasing heave fidelity when pitch motion is also available. These two trends are responsible for the statistically significant effect of the supplied motion on the pilot motion gain [$F(8, 48) = 30.88$, $p < 0.05$]. Post-hoc analysis indeed revealed that no significant differences in K_m were present for the conditions without pitch motion (black data in Fig. 14d).

Despite the fact that changes in both pilot-model time delays appear to be relatively modest (from Figs. 14e and 14f), the ANOVAs performed on the values found for both parameters revealed these changes are significant effects: $F(1, 6) = 10.43$, $p < 0.05$ and $F(4, 24) = 5.73$, $p < 0.05$ for the main effects of pitch and heave motion on τ_v, respectively; $F(1, 6) = 10.69$, $p < 0.05$ for the effect of the overall variation in supplied motion on τ_m. Both delays are found to be slightly higher for the conditions for which pitch motion was available. In addition, a decreasing trend in τ_m with increasing heave fidelity can be observed, from Fig. 14f.

The final two pilot-model parameters, shown in Fig. 14, are the neuromuscular system eigenfrequency ω_{nm} and the damping factor ζ_{nm}. The neuromuscular frequency is found to increase both with the addition of pitch motion and with increasing heave fidelity. Despite the relatively large error bars, shown in Fig. 14g, both these effects were statistically significant: $F(1, 6) = 22.01$, $p = 0.003$ and $F(1.60, 9.59) = 5.04$, $p = 0.037$ for pitch and heave, respectively. Such increases in ω_{nm} with increasing motion strength have also been reported for other experiments [10,20]. As can be judged from Table 6, no significant main effects were found for the neuromuscular system damping factor ζ_{nm}.

V. Discussion

Seven subjects participated in an experiment investigating the effects of heave washout settings on pilot performance and control behavior in a pitch attitude disturbance-rejection task. The effect of heave motion fidelity was investigated by independently adjusting the gain and break frequency of a third-order linear washout filter. All heave motion conditions were performed with and without additional rotational pitch motion. The current experiment has shown that the relatively small impact of pitch-heave on pilot control behavior, compared with rotational pitch motion found in [10], was a result of the heave washout filter used in that study. Here, almost equal performance and pilot control behavior were observed for the conditions with only rotational pitch and only one-to-one pitch-heave motion, as expected from the linear relation between both motion cues.

Table 6 Two-way repeated measures ANOVA results for neuromuscular system model parameters, where ** is highly significant ($p < 0.05$), * is significant ($0.05 \leq p < 0.1$), and - is not significant ($p \geq 0.1$)

Independent variables	Dependent measures					
	ω_{nm}			ζ_{nm}		
Factor	df	F	Sig.	df	F	Sig.
Pitch	1, 6	22.01	**	1, 6	0.37	-
Heave	1.6, 9.6[a]	5.04	**	1.4, 8.7	1.72	-
Pitch × heave	4, 24	2.67	*	4, 24	2.99	*

[a]Greenhouse–Geisser sphericity correction.

Pilot performance and control activity are found to be significantly reduced if the heave motion is attenuated using a washout filter. If rotational pitch motion is available, the reduction is markedly smaller. The presence of washout is seen to degrade performance and control activity more than pure gain attenuation. In addition, the control strategy of the pilot is found to be significantly affected when heave motion is attenuated, as seen by a change in disturbance and target crossover frequencies and phase margins. The disturbance crossover frequency is significantly increased when the fidelity of the heave motion is increased.

This change in control strategy is also reflected by significant changes in the identified pilot-model parameters. With increasing heave motion fidelity, the visual and motion perception gains of the pilot model are seen to increase while the visual lead decreases. The increase in motion perception gain and the decrease in visual lead constant observed for conditions with increased heave motion fidelity indicate that pilots will clearly prefer the availability of lead information from these heave motion cues. Additionally, by increasing heave motion fidelity, the visual and physical motion perception time delays increase and decrease, respectively. This is further evidence of an increase in the usefulness of the motion cues when the fidelity is increased. Crossover frequencies, phase margins, and pilot-model parameters show similar trends with and without additional pitch motion.

The conditions with washout on the supplied heave motion (F0.6 and F1.0) show some interesting results for the pilot visual lead in addition to the observed global trends. The visual lead for these conditions is lower compared with the conditions for which the heave motion is attenuated with only a gain. This could be explained by the fact that extra lead information is present due to the high-pass washout filter characteristics, as can be seen in Fig. 2. The extra lead information reduces the need for the pilot to generate extra lead, allowing the visual lead constant to be reduced. However, this effect on the generated visual lead does not seem to affect the remaining dependent measures.

Overall, it can be concluded that all attenuation of the heave motion as considered in this experiment resulted in changes in pilot control behavior. Even a reduction in heave motion gain to a value of 0.6, which is still stated to be quite acceptable in some publications, already shows significant degradation of tracking performance, pilot crossover frequency, and the contribution of motion feedback to pilot control behavior (as indicated by a reduction in the pilot-model motion perception gain). The effect of the phase attenuation caused by the addition of heave washout is clearly seen to further increase this discrepancy in pilot control behavior with respect to the condition with one-to-one heave motion. Though lower in magnitude, these effects of heave motion fidelity are still observable even when additional one-to-one pitch motion cues are available. As, within the limitations of the current experiment, the conditions for which both pitch and pitch-heave motion were presented one-to-one are arguably the most representative of real flight, these findings suggest that it is highly preferable to present motion cues that pilots might rely on in continuous aircraft control tasks at the highest achievable level of motion fidelity.

Only part of the total vertical aircraft motion that occurs during pitch maneuvering was, however, considered in the current study. Heave motion originating from movement of the aircraft c.g. was not simulated in the current experiment, as it can not be represented one-to-one. Based on the findings of [10], c.g. heave is hypothesized to act as a disturbance on the remaining motion components during pitch control and could therefore degrade pilot tracking performance compared with the condition with one-to-one rotational pitch and pitch-heave motion. In that experiment, a nonsignificant decrease in performance was observed with the addition of filtered c.g. heave motion in addition to a surprising increase in the amount of lead pilots generated visually (that is, opposite effects to those found for pitch and pitch-heave motion). The addition of this c.g. heave could therefore result in different results on the effects of pitch-heave and rotational pitch motion on pilot performance and control behavior as described in this paper. Future experiments, in which pilot control behavior for tracking tasks similar to the one described here will be

compared in real flight and in the simulator, are expected to show how the effects of simulator washout measured in the current experiment compare to true in-flight pilot control behavior.

The pilot model used in the present study contains a generic motion perception channel with only a lead term. This motion perception channel is applied for modeling both the perception of heave and rotational pitch motion, as both are shown to effectively yield additional pilot lead. In the case of heave motion, only a factor is added to compensate for the distance between the c.g. and the pilot station. The proposed model proved to be accurate in replicating the measured time-domain data, as is indicated by the high VAF for all conditions. Furthermore, due to the difficulty in separating pilot responses to the proprioceptive, somatosensory, and vestibular stimuli that result from physical motion cueing, the physical pilot models described in literature often attribute the total pilot motion response to the dominant motion sensor (that is, the vestibular system for rotational motion). Alternatively, the generic model used in this study lumps all separate contributions together in a single generic model structure, which may be a preferred approach in future experiments on pilot modeling.

The current study was performed for a Cessna Citation I aircraft, which has a relatively small distance of 3.2 m between the c.g. and the pilot station, whereas for typical airliners, this distance can be more than 10 times larger. This also yields a much higher magnitude of the pitch-heave component for an airliner compared with the small aircraft used in this experiment. In some dependent measures, such as pilot performance, the trend in the data as a result of the heave motion attenuation was reduced when rotational pitch motion was present. This may suggest that rotational pitch motion is more dominant than pitch-heave motion if both are present. If the pitch-heave motion is larger in magnitude, however, the trend as a result of the pitch-heave attenuation could also be more pronounced when rotational pitch motion is present. This topic may be covered in future research.

VI. Conclusions

An experiment was performed to investigate how pilot performance and control behavior in an aircraft pitch control task are affected by attenuation of the associated heave motion by a high-pass washout filter. When both are presented one-to-one, the effects of pitch and heave motion on pilot control behavior were found to be highly similar. Pilot performance and control activity are found to be significantly reduced, however, when the heave motion is filtered or only attenuated with a gain. This reduction is smaller in magnitude if rotational pitch motion is available in addition to the heave motion. The additional phase attenuation caused by the washout clearly affects tracking performance and pilot control behavior more than pure gain attenuation. The changes in crossover frequencies and phase margins, and the pilot-model parameters show that if the fidelity of the heave motion is increased, pilots will rely more on these motion cues to improve their task performance. This is mainly reflected by an increase in visual and motion perception gains and a decrease in pilot visual lead.

Acknowledgments

This research was supported by The Netherlands Technology Foundation (STW), the applied science division of The Netherlands Organization for Scientific Research (NWO), and the technology program of the Ministry of Economic Affairs.

References

[1] Schmidt, S. F., and Conrad, B., "Motion Drive Signals for Piloted Flight Simulators," NASA CR-1601, 1970.

[2] Grant, P. R., and Reid, L. D., "Motion Washout Filter Tuning: Rules and Requirements," *Journal of Aircraft*, Vol. 34, No. 2, 1997, pp. 145–151. doi:10.2514/2.2158

[3] Ringland, R. F., and Stapleford, R. L., "Motion Cue Effects on Pilot Tracking," *Seventh Annual Conference on Manual Control*, SP-281, NASA, Washington D.C., 1971, pp. 327–338.

[4] Jex, H. R., Magdaleno, R. E., and Junker, A. M., "Roll Tracking Effects of G-Vector Tilt and Various Types of Motion Washout," *Fourteenth Annual Conference on Manual Control*, NASA Ames Research Center, Moffet Field, CA, 1978, pp. 463–502.

[5] Reid, L. D., and Nahon, M. A., "Flight Simulation Motion-Base Drive Algorithms Part 3: Pilot Evaluations," TR 319, Univ. of Toronto Inst. for Aerospace Studies, Toronto, 1986.

[6] Schroeder, J. A., "Helicopter Flight Simulation Motion Platform Requirements," TP 1999-208766, NASA, 1999.

[7] Gouverneur, B., Mulder, J. A., Van Paassen, M. M., Stroosma, O., and Field, E. J., "Optimisation of the SIMONA Research Simulator's Motion Filter Settings for Handling Qualities Experiments," AIAA Modeling and Simulation Technologies Conference and Exhibit, AIAA No. 2003-5679, 2003.

[8] Telban, R. J., Cardullo, F. M., and Kelly, L. C., "Motion Cueing Algorithm Development: Piloted Performance Testing of the Cueing Algorithms," NASA CR 2005-213748, 2005.

[9] Hosman, R. J. A. W., Van de Moesdijk, G. A. J., and Van der Vaart, J. C., "Optimalization and Evaluation of Linear Motion Filters," *Fifteenth Annual Conference on Manual Control*, Wright State Univ., Dayton, OH, 20–22 March 1979, pp. 213–242.

[10] Zaal, P. M. T., Pool, D. M., De Bruin, J., Mulder, M., and Van Paassen, M. M., "Use of Pitch and Heave Motion Cues in a Pitch Control Task," *Journal of Guidance, Control, and Dynamics*, Vol. 32, No. 2, 2009, pp. 366–377. doi:10.2514/1.39953

[11] Field, E. J., Armor, J. B., and Rossitto, K. F., "Effects of Pitch Instantaneous Center of Rotation Location on Flying Qualities," AIAA Modeling and Simulation Technologies Conference and Exhibit, AIAA No. 2002-4799, 2002.

[12] McRuer, D. T., Graham, D., Krendel, E. S., and Reisener, W., Jr., "Human Pilot Dynamics in Compensatory Systems. Theory, Models and Experiments with Controlled Element and Forcing Function Variations," AFFDL-TR-65-15, U.S. Air Force Flight Dynamics Lab., Wright-Patterson Air Force Base, OH, Aug, 1965.

[13] McRuer, D. T., and Jex, H. R., "A Review of Quasi-Linear Pilot Models," *IEEE Transactions on Human Factors in Electronics*, Vol. HFE-8, No. 3, 1967, pp. 231–249. doi:10.1109/THFE.1967.234304

[14] McRuer, D. T., and Krendel, E. S., "Mathematical Models of Human Pilot Behavior," AG188, AGARD, Jan, 1974.

[15] Van der Vaart, J. C., "Modelling of Perception and Action in Compensatory Manual Control Tasks," Ph.D. Thesis, Delft Univ. of Technology, Faculty of Aerospace Engineering, Delft, The Netherlands, 1992.

[16] Hosman, R. J. A.W., "Pilot's Perception and Control of Aircraft Motions," Ph.D. Thesis, Delft University of Technology, Faculty of Aerospace Engineering, Delft, The Netherlands, 1996.

[17] Zaal, P. M. T., Pool, D. M., Chu, Q. P., Van Paassen, M. M., Mulder, M., and Mulder, J. A., "Modeling Human Multimodal Perception and Control Using Genetic Maximum Likelihood Estimation," *Journal of Guidance, Control, and Dynamics*, Vol. 32, No. 4, 2009, pp. 1089–1099. doi:10.2514/1.42843

[18] Nieuwenhuizen, F. M., Zaal, P. M. T., Mulder, M., Van Paassen, M. M., and Mulder, J. A., "Modeling Human Multi-Channel Motion Perception and Control Using Linear Time-Invariant Models," *Journal of Guidance, Control, and Dynamics*, Vol. 31, No. 4, 2008, pp. 999–1013. doi:10.2514/1.32307

[19] Pool, D. M., Zaal, P. M. T., Damveld, H. J., Van Paassen, M. M., and Mulder, M., "Pilot Equalization in Manual Control of Aircraft Dynamics," *Proceedings of the 2009 IEEE International Conference on Systems, Man, and Cybernetics*, Inst, of Electrical and Electronics Engineers, Piscataway, NJ, 2009.

[20] Pool, D. M., Zaal, P. M. T., Mulder, M., Van Paassen, M. M., and Mulder, J. A., "Parameter Estimation of Multimodal Pilot Models for Manual Target-Following Tasks," *Proceedings of the 27th European Annual Conference on Human Decision-Making and Manual Control*, Delft Univ. of Technology, Delft, The Netherlands, 2008.

[21] Praamstra, F. J., Zaal, P. M. T., Pool, D. M., Ellerbroek, J., Mulder, M., and Van Paassen, M. M., "Function of Attitude Perception in Human Control Behavior in Target Tracking Tasks," Proceedings of the AIAA Modeling and Simulation Technologies Conference and Exhibit, AIAA No. 2008-6845, 2008.

[22] Zaal, P. M. T., Pool, D. M., Mulder, M., and Van Paassen, M. M., "Multimodal Pilot Control Behavior in Combined Target-Following Disturbance-Rejection Tasks," *Journal of Guidance, Control, and Dynamics*, Vol. 32, No. 5, 2009, pp. 1418–1428. doi:10.2514/1.44648

[23] Hosman, R. J. A. W., Grant, P., and Schroeder, J. A., "Pre and Post Pilot Model Analyis Compared to Experimental Simulator Results," AIAA

Modeling and Simulation Technologies Conference and Exhibit, AIAA No. 2005-6303, 2005.

[24] Berkouwer, W. R., Stroosma, O., Van Paassen, M. M., Mulder, M., and Mulder, J. A., "Measuring the Performance of the SIMONA Research Simulator's Motion System," AIAA Modeling and Simulation Technologies Conference and Exhibit, AIAA No. 2005-6504, 2005.

[25] Stroosma, O., Van Paassen, M. M., Mulder, M., and Postema, F. N., "Measuring Time Delays in Simulator Displays," AIAA Modeling and Simulation Technologies Conference and Exhibit, AIAA No. 2007-6562, 2007.

[26] Steurs, M., Mulder, M., and Van Paassen, M. M., "A Cybernetic Approach to Assess Flight Simulator Fidelity," AIAA Modeling and Simulation Technologies Conference and Exhibit, AIAA No. 2004-5442, 2004.

[27] Dehouck, T. L., Mulder, M., and Van Paassen, M. M., "The Effects of Simulator Motion Filter Settings on Pilot Manual Control Behaviour," AIAA Modeling and Simulation Technologies Conference and Exhibit, AIAA No. 2006-6250, 2006.

[28] Pool, D. M., Mulder, M., Van Paassen, M. M., and Van der Vaart, J. C., "Effects of Peripheral Visual and Physical Motion Cues in Roll-Axis Tracking Tasks," *Journal of Guidance, Control, and Dynamics*, Vol. 31, No. 6, 2008, pp. 1608–1622. doi:10.2514/1.36334

[29] Van Paassen, M. M., and Mulder, M., "Identification of Human Operator Control Behaviour in Multiple-Loop Tracking Tasks," *Proceedings of the Seventh IFAC/IFIP/IFORS/IEA Symposium on Analysis, Design, and Evaluation of Man-Machine Systems*, Pergamon, Oxford, 1998, pp. 515–520.